

Normal coordinate analysis of the copper center of azurin and the assignment of its resonance Raman spectrum

(blue copper proteins/coordination geometry/bond force constants/vibrational spectroscopy)

THOMAS J. THAMANN*[†], PATRICK FRANK[‡]§, LAWRENCE J. WILLIS*[¶], AND THOMAS M. LOEHR*[¶]

*Department of Chemistry and Biochemical Sciences, Oregon Graduate Center, Beaverton, Oregon 97006; and [‡]Department of Chemistry, Stanford University, Stanford, California 94305

Communicated by Harry B. Gray, June 28, 1982

ABSTRACT Normal coordinate analysis that utilizes a general valence force field and the Wilson FG matrix method has been applied to several structural models representing the active site of the blue copper protein, azurin. The models included tetrahedral and square planar $\text{CuN}_2\text{SS}'$, trigonal CuN_2S , and trigonal bipyramidal $\text{CuN}_2\text{SS}'\text{O}$ structures in which the Ns are imidazole nitrogens of histidines, S is the thiolate sulfur of cysteine, S' is the thioether sulfur of methionine, and O is a peptide carbonyl oxygen. For constant Cu—ligand bond lengths and initial force constants, the force field was refined against the most intense of the observed frequencies (424, 404, 369, and 261 cm^{-1}) in the resonance Raman spectrum of *Pseudomonas aeruginosa* azurin. The most satisfactory fit between observed and calculated frequencies occurs for tetrahedral and trigonal structures. The calculations provide detailed assignments for the resonance Raman spectrum of azurin and reveal considerable mixing of Cu—S(Cys) and Cu—N(His) vibrational modes. The trigonal model is favored because it is shown that the $\approx 260\text{-cm}^{-1}$ vibration is an invariant feature in the resonance Raman spectra of blue copper proteins, even those lacking a methionine in the vicinity of the copper atom. The present analysis ascribes the high frequencies of the Cu—ligand stretching modes and the resonance enhancement to the coupled nature of their vibrations and the Franck–Condon overlaps with predominant (Cys)S→Cu(II) charge transfer bands in the visible region.

The assignments of the resonance Raman spectra of the type 1 site in blue copper proteins have not yet been unambiguously established. Several laboratories have investigated these proteins and observed that excitation into their characteristic absorption bands near 625 nm produces quite similar resonance Raman spectra (1–5). Both the single copper proteins such as azurin, plastocyanin, and stellacyanin and the multi-copper proteins ascorbate oxidase, ceruloplasmin, and laccase exhibit a series of strong peaks in the 350- to 430-cm^{-1} region, along with a number of weak peaks on either side of this interval. Recent advances in the structural elucidation of the copper sites of azurin and plastocyanin have helped to establish the presence of two histidine N atoms, one cysteine S atom, and, possibly, one methionine S atom as the most likely ligands in a nearly tetrahedral arrangement (6–13). Thus, it has become imperative to develop an understanding of the resonance Raman data and their correspondence to the emerging structural description of the copper center.

Several troublesome features have hampered a thorough assignment of the resonance Raman data. (i) The observed frequencies are unusually high for Cu(II)—N(imidazole) and Cu(II)—S(thiolate) bonding by reference to the frequencies of other metalloproteins or model complexes. For example, Cu(II)—N(His) vibrations in hemocyanin and tyrosinase have

been assigned to frequencies at $220\text{--}320\text{ cm}^{-1}$ (14, 15). Cu(II)—S vibrations in complexes are often regarded to be even lower in frequency (16), although more recent work on metal-dithiocarbamates and metal-thiolates suggests that these frequencies may lie as high as 400 cm^{-1} (17–19). (ii) The assignment of the $\approx 260\text{-cm}^{-1}$ peak appearing in all blue copper proteins as the Cu(II)—S(Met) stretching mode is in agreement with the observation of peaks near 270 cm^{-1} in the Raman spectra of copper-polythiaether complexes (20) but does not account for the absence of methionine in stellacyanin (21). The 267-cm^{-1} peak in stellacyanin has been rationalized as a possible Cu(II)—disulfide vibration (20). Furthermore, refined crystallographic data on plastocyanin (22) as well as extended x-ray absorption fine structure (EXAFS) results on azurin (10) have revealed that the Cu—S(Met) distance is likely to be as much as 2.9 \AA , calling into question the veracity of the proposed assignment of the Raman band at $\approx 260\text{ cm}^{-1}$. (iii) The resonance Raman spectra of the blue copper proteins also have been considered to be compatible with oxygen coordination (1, 2), peptide nitrogen coordination (1), and a trigonal bipyramidal five-coordinate geometry (2) of the metal center.

To address these inconsistencies and to test the dependence of the Cu(II)—ligand frequencies upon structural and bond force constant variations, we have undertaken normal coordinate analysis using data from the resonance Raman spectrum of the *Pseudomonas aeruginosa* blue protein, azurin. Active site complexes of the type CuN_2S_2 , CuN_2S (the formulation for the center where the methionine S atom is beyond bonding distance), and $\text{CuN}_2\text{S}_2\text{O}$ were tested. We anticipated that the results of these calculations would permit an elucidation of the azurin active site structure vis-à-vis the higher resolution plastocyanin structure presently available.

EXPERIMENTAL

Azurin from *P. aeruginosa* was isolated and purified by standard procedures with a purity equal to or exceeding literature values (23, 24). Resonance Raman data on azurin were obtained by signal averaging on a computer-controlled laser Raman spectrophotometer; this modified instrument has been described in detail elsewhere (25). The sample was maintained at $\approx 2^\circ\text{C}$ by contact between the glass capillary containing the sample with a hollowed-out copper rod immersed in a Dewar flask holding an ice-water mixture. Normal coordinate analyses utilizing the Wilson FG matrix method (26, 27) and a general valence force field were carried out on a PRIME 350 computer

Abbreviation: EXAFS, extended x-ray absorption fine structure.

[†] Present address: Pharmaceutical Research and Development, The Upjohn Company, Kalamazoo, MI 49001.

[§] Present address: Dept. Chemical Immunology, The Weizmann Institute of Science, Rehovot, Israel 76100.

[¶] To whom reprint requests should be addressed.

The publication costs of this article were defrayed in part by page charge payment. This article must therefore be hereby marked "advertisement" in accordance with 18 U. S. C. §1734 solely to indicate this fact.

system by using the Schachtschneider computational programs obtained from the National Research Council of Canada (28). The use of this program was described in our recent study of Cu(II,III) complexes of biuret and oxamide (29).

RESULTS AND DISCUSSION

Observed Raman Spectrum. The resonance Raman spectrum of *P. aeruginosa* azurin in the frequency interval 600–100 cm^{-1} is shown in Fig. 1. Reduction of azurin with dithionite results in a loss of color and elimination of all the Raman spectral peaks in this frequency region (Fig. 1, lower trace). The oxidized azurin spectrum contains three intense peaks at 424, 404, and 369 cm^{-1} , two weaker, broad peaks at 261 and 115 cm^{-1} , as well as many weak bands between 500 and 100 cm^{-1} . Because all of the peaks in this region appear to be resonance-enhanced, the observed spectrum would be expected to arise from vibrational motions of the copper chromophore and the most intense peaks should be due to Cu—ligand stretching modes.

Identical Raman shifts and intensities were observed when 568.2-, 647.1-, or 676.4-nm excitation was employed. When 530.9-nm or 488.0-nm excitation was used, only the three strongest features at 424, 404, and 369 cm^{-1} were clearly observed; although the overall quality was considerably poorer, no changes in relative intensities among these peaks were noted. Excitation with the 406.7-nm line in the near-UV resulted in bleaching of the chromophore within a few minutes.

Normal Coordinate Analysis: Initialization. Normal coordinate analysis requires a structural model, a set of observed spectral frequencies, and a force field—i.e., a set of force constants for stretching and deformation modes of vibration. The program then optimizes calculated frequencies by refinement of force constants. The structural model for beginning this analysis was based upon early crystallographic and spectroscopic results that indicated a Cu—N₂SS' ligand set of approximate tetrahedral geometry. The bond lengths chosen for this analysis were those taken from EXAFS data analyses for two Cu—N distances of 1.97 Å, a short Cu—S(Cys) of 2.10 Å, and a long Cu—S(Met) of ≈ 2.75 Å (ref. 10; T. Tullius and K. O. Hodgson, personal communication). Our initial choices of force constants were those typically found for divalent Cu and Ni complexes with N and S ligands (29, 30–33). It should be noted that the N ligands present a unique problem because they belong to im-

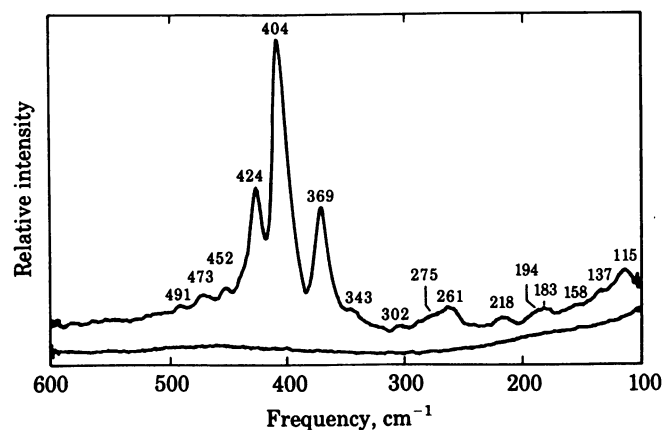


FIG. 1. The upper trace shows a resonance Raman spectrum of *P. aeruginosa* azurin (≈ 1 mM, in 0.05 M ammonium acetate, pH 6.0) obtained with 647.1-nm excitation (120 mW at the Dewar containing the sample) in a backscattering geometry. The sample was maintained at $\approx 2^\circ\text{C}$ for 67 repetitive scans, each at a scan rate of 2.0 cm^{-1}/s , slitwidth of 4.5 cm^{-1} , and a digitizing increment of 0.5 cm^{-1} . The lower trace shows a Raman spectrum of dithionite-reduced azurin under identical conditions (56 scans). Both spectra have been subjected to a 25-point smooth.

idazole rings of coordinated histidines. These rings generally behave as “stiff” ligands in metal complexation, having an effective mass of ≈ 65 atomic mass units, and account for the typical frequencies of metal—imidazole vibrations at 280–250 cm^{-1} (34). However, unreasonable force constants would be required to push these frequencies as high as 430–370 cm^{-1} , as observed in the blue copper proteins. For this reason, we treated the coordinated N as a mass of 14 atomic mass units and utilized typical Cu—N force constants. Finally, the initial trial set of force constants was refined against four of the observed frequencies, including the three most intense peaks (424, 404, and 369 cm^{-1}) and the higher frequency component of the two broad bands (261 cm^{-1}) which had been proposed (20) to be due to the Cu—S(Met) vibration. For each model, $3n - 6$ frequencies are calculated even though only four observed values are provided for the computations.

Tetrahedral CuN₂S₂ Models. Both regular and tetragonally distorted tetrahedral models were considered for the CuN₂S₂ formulation. Skeletal frequencies were found to be relatively unaffected by small tetragonal distortions up to bond angles of 121.5°. Similarly, trigonally distorted CuN₂S₂ structures were investigated for Cu atom distances of 0.15, 0.25, 0.50, 0.75, and 1.0 Å above the N₂S(Cys) plane. The 0.75-Å distance gave the best fit of calculated-to-observed frequencies and this structure has essentially tetrahedral bond angles. Thus, only the calculated frequencies and band assignments for an *average* tetrahedral structure are given in Table 1. The refined force constants for this initial model are given in Table 2.

The refined force field provides an excellent fit to the four observed frequencies specified. In addition, five other values are calculated that closely match other frequencies in the resonance Raman spectrum of azurin and are reasonably assigned as deformation modes. With the exception of the 424- cm^{-1} band, all calculated frequencies show evidence of considerable mixing of vibrational contributions, and in particular, are seen by inspection of Table 1 to involve the Cu—S(Cys) coordinate. The mixing with the Cu—S(Cys) mode accounts nicely for the observed enhancement of their intensities because resonance is achieved by excitation within the (Cys)S→Cu(II) charge transfer band (13). The 369- cm^{-1} band is largely the Cu—S(Cys) vibration, whereas the other two intense peaks have predominantly $\nu(\text{Cu—N})$ character. As expected from the lower value of the Cu—S(Met) force constant provided at the outset, the 261- cm^{-1} band is ascribed principally to $\nu(\text{Cu—S(Met)})$. Ferris *et al.* (5) arrived at a similar interpretation based on their observation of higher energy peaks in the *P. aeruginosa* azurin spectrum. They attributed features at 814, 780, and 748 cm^{-1} to an overtone of the 407- cm^{-1} band, a combination of the 407- and 372- cm^{-1} bands, and an overtone of the 372- cm^{-1} band, respectively. With no evidence for a spectral feature at ≈ 850 cm^{-1} ($= 2 \times 425$ cm^{-1}), they assigned their 425- cm^{-1} peak as a predominantly Cu—N(His) vibration. The present normal coordinate analysis results for a tetrahedral CuN₂S₂ model provide a theoretical framework for their proposed assignments (5). Not only are the calculated frequencies for this model in excellent agreement with many of the observed values but also the refined force constants are satisfactory.

Alternate Structural Models. Provided with a “satisfactory fit” for the tetrahedral structural type, we investigated the sensitivity of the calculations to other coordination geometries of the model. Various structures were chosen to represent typical Cu(I) and Cu(II) complexes as well as those suggested for the type 1 site; they included trigonal, trigonal bipyramidal, and square planar models. To maximize the diagnostic value of this theoretical approach we have fixed all bond lengths, initial force constants (the refined values from the tetrahedral case were used), and the same four observed frequencies. Only the geo-

Table 1. Frequencies and band assignments for the CuN_2S_2 tetrahedral model and for a trigonal CuN_2S model with the Cu atom 0.75 Å above the ligand plane

| Obs., cm^{-1} * | Tetrahedral CuN_2S_2 | | Trigonal CuN_2S | |
|--------------------------|--------------------------------------|---|---------------------------------|---|
| | Calc., cm^{-1} | Band assignments | Calc., cm^{-1} | Band assignments |
| 424 s | 424 | 97% $\nu(\text{Cu—N})$ | 424 | 93% $\nu(\text{Cu—N})$ + 3% $\nu(\text{Cu—S})$ |
| 404 vs | 404 | 81% $\nu(\text{Cu—N})$ + 17% $\nu(\text{Cu—S}_1)$ | 405 | 67% $\nu(\text{Cu—N})$ + 30% $\nu(\text{Cu—S})$ |
| 369 s | 370 | 62% $\nu(\text{Cu—S}_1)$ + 15% $\nu(\text{Cu—N})$ + 11% $\nu(\text{Cu—S}_2)$ | 368 | 57% $\nu(\text{Cu—S})$ + 35% $\nu(\text{Cu—N})$ |
| 343 w | | | | |
| 302 w | | | | |
| 275 sh, w | | | | |
| 261 m | 260 | 58% $\nu(\text{Cu—S}_2)$ + 19% $\nu(\text{Cu—S}_1)$ + 11% $\delta(\text{N—Cu—S}_1)$ | 260 | 92% $\delta(\text{S—Cu—N})$ |
| 218 w | 210 | 80% $\delta(\text{N—Cu—S}_1)$ + 19% $\delta(\text{N—Cu—S}_2)$ | 226 | 92% $\delta(\text{S—Cu—N})$ |
| 194 sh, w | 202 | 41% $\delta(\text{N—Cu—S}_1)$ + 30% $\nu(\text{Cu—S}_2)$ + 27% $\delta(\text{N—Cu—S}_2)$ | | |
| 183 w | | | | |
| 158 vw | 160 | 80% $\delta(\text{N—Cu—S}_2)$ + 18% $\delta(\text{N—Cu—S}_1)$ | | |
| 137 vw | 130 | 37% $\delta(\text{N—Cu—S}_2)$ + 35% $\delta(\text{N—Cu—N})$ + 22% $\delta(\text{Cu—S}_1)$ | | |
| 115 m | 102 | 69% $\delta(\text{S}_1\text{—Cu—S}_2)$ + 27% $\delta(\text{N—Cu—N})$ | 91 | 99% $\delta(\text{N—Cu—N})$ |

S_1 = sulfur at 2.10 Å and S_2 = sulfur at 2.75 Å; for the trigonal model S_2 is considered to be beyond bonding distance of copper; for this computation, all force constants involving S_2 of the corresponding CuN_2S_2 trigonal model were set equal to zero.

* v, Very; s, strong; m, medium; w, weak; sh, shoulder.

metrical structures (and in one case the identities of the ligand atoms) were varied. As before, the goodness of fit in each case was determined from a comparison of the observed and calculated frequencies (Tables 1 and 3) and from the suitability of the refined force constants (Table 2).

Trigonal $\text{CuN}_2\text{S}(\text{Cys})$. This model includes the possibility that the methionine is beyond bonding distance. As for the tetrahedral prototype, calculated frequencies were sensitive to the Cu elevation above the ligand plane. Good agreement was only obtained for Cu distances of 0.50 and 0.75 Å above the trigonal plane and the data for the 0.75-Å case are presented in Tables 1 and 2. Although only six frequencies characterize this four-atom structure, the contributions of normal modes to the three intense spectral features are satisfactory, revealing considerable Cu—N and Cu—S mixing among the two lower frequency components. The 260- cm^{-1} peak is assigned here to a S—Cu—N deformation mode, and thus, quite likely to be of low intensity. However, this apparent overall good fit is rendered less than satisfactory because both S—Cu— N_1 and S—Cu— N_2 bending force constants refined to values of 120 and 100 $\text{N}\cdot\text{m}^{-1}$, respectively; their average value of 110 $\text{N}\cdot\text{m}^{-1}$ (Table 2) is judged to be too high because it is equivalent to the value of $\text{K}(\text{Cu—N})$.

Square Planar CuN_2S_2 . *Cis-* and *trans-* CuN_2S_2 geometries yielded similar results, and the values calculated for the *cis* structure are given in Tables 2 and 3. However, the match between observed and calculated frequencies is not good. All at-

tempts to obtain calculated frequencies at both 424 and 369 cm^{-1} failed, although a band matching the 404- cm^{-1} feature could be obtained. Table 3 shows the best intermediate values. The square planar CuN_2S_2 model predicts significant Cu—S and Cu—N mixing for the outer pair of the intense spectral peaks, but the potential energy matrix for this force field weighs their contributions equally and therefore keeps their frequency difference at a fixed value. This calculated difference of 100 cm^{-1} is considerably greater than the observed value of 55 cm^{-1} for these modes. Therefore, it would be impossible to fit both the 369- and 424- cm^{-1} frequencies with the refined force field.

Trigonal Bipyramidal $\text{CuN}_2\text{S}_2\text{O}$. In this model, the coordination sphere is expanded to include a carbonyl oxygen at a distance of 2.5 Å from the Cu atom. This geometry was suggested during the early stages of refinement of the azurin structure from *Alcaligenes dentrificans* (G. E. Norris, B. F. Anderson, and E. N. Baker, personal communication) and the presence of such an oxygen has similarly been suggested by O. Farver (personal communication) in viewing the coordinates obtained by Adman *et al.* (8). For *P. aeruginosa* azurin, the presence of an amide carbonyl ligand has also been suggested from ^{13}C NMR spectra (35). All other Cu—ligand distances have been held fixed as in the earlier models. The choice of initial force constants for modes involving the O atom were based upon the refined values for Cu—N modes emanating from the tetrahedral structure. They were 100 $\text{N}\cdot\text{m}^{-1}$ for $\text{K}(\text{Cu—O})$, 50 $\text{N}\cdot\text{m}^{-1}$ for $\text{H}(\text{S}_1\text{—Cu—O})$, and 20 $\text{N}\cdot\text{m}^{-1}$ for $\text{H}(\text{N—Cu—O})$ and were allowed to refine to the values shown in Table 2. The results of the assignments for this model are given in Table 3, but they, too, do not appear to be satisfactory. For example, there is little mixing of vibrational modes among the principal bands. Furthermore, the value of the refined $\text{K}[\text{Cu—S}(\text{Cys})]$ is depressed so far that the frequency for this stretching vibration ends up at 262 cm^{-1} , and the weak resonance enhancement of this peak makes its assignment to $\nu[\text{Cu—S}(\text{Cys})]$ unreasonable. Moreover, the dominant band at 369 cm^{-1} is here attributed to the distant O and S ligands.

Review of Trial Models and Refinements. Normal coordinate analysis appears able to provide a structure-sensitive approach to a description of the resonance Raman spectrum of *P. aeruginosa* azurin for which no detailed assignments have heretofore been provided. Despite the considerable difficulty in choosing a "correct" force field, the choice of consistent input values to the computation has yielded a good fit of frequencies and reasonable assignments for tetrahedral and trigonal models,

Table 2. Refined force constants ($\text{N}\cdot\text{m}^{-1}$) for the molecular models

| Mode | Tetrahedral CuN_2S_2 | Trigonal CuN_2S | Square planar CuN_2S_2 | Trigonal bipyramidal $\text{CuN}_2\text{S}_2\text{O}$ |
|--------------------------------------|--------------------------------------|---------------------------------|--|---|
| Stretch | | | | |
| $\text{K}(\text{Cu—N})$ | 110 | 110 | 100 | 110 |
| $\text{K}(\text{Cu—S}_1)$ | 160 | 170 | 190 | 86 |
| $\text{K}(\text{Cu—S}_2)$ | 84 | | 93 | 83 |
| $\text{K}(\text{Cu—O})$ | | | | 94 |
| Bend | | | | |
| $\text{H}(\text{N—Cu—N})$ | 12 | 11 | 12 | 17 |
| $\text{H}(\text{N—Cu—S}_1)$ | 68 | 110 | 39 | 38 |
| $\text{H}(\text{N—Cu—S}_2)$ | 59 | | 44 | 28 |
| $\text{H}(\text{S}_1\text{—Cu—S}_2)$ | 29 | | 21 | 31 |
| $\text{H}(\text{S}_1\text{—Cu—O})$ | | | | 51 |
| $\text{H}(\text{N—Cu—O})$ | | | | 18 |

No force constants were held fixed during refinements.

Table 3. Frequencies and band assignments for the CuN₂S₂ square planar model and for the CuN₂S₂O trigonal bipyramidal model

| Square planar CuN ₂ S ₂ | | | Trigonal bipyramidal CuN ₂ S ₂ O | |
|---|-------------------------|--|--|--|
| Obs., cm ⁻¹ * | Calc., cm ⁻¹ | Band assignments | Calc., cm ⁻¹ | Band assignments |
| 424 s | 441 | 50% $\nu(\text{Cu—S}_1)$ + 48% $\nu(\text{Cu—N})$ | 430 | 97% $\nu(\text{Cu—N})$ |
| 404 vs | 405 | 90% $\nu(\text{Cu—N})$ + 9% $\nu(\text{Cu—S}_2)$ | 397 | 93% $\nu(\text{Cu—N})$ |
| 369 s | 341 | 51% $\nu(\text{Cu—N})$ + 49% $\nu(\text{Cu—S}_1)$ | 369 | 86% $\nu(\text{Cu—O})$ + 12% $\nu(\text{Cu—S}_2)$ |
| 343 w | | | | |
| 302 w | | | | |
| 275 sh, w | | | | |
| 261 m | 261 | 87% $\nu(\text{Cu—S}_2)$ + 10% $\nu(\text{Cu—N})$ | 262 | 84% $\nu(\text{Cu—S}_1)$ |
| 218 w | | | | |
| 194 sh, w | | | | |
| 183 w | | | 170 | 96% $\delta(\text{S}_1\text{—Cu—N})$ |
| 158 vw | 154 | 38% $\delta(\text{S}_1\text{—Cu—N})$ + 32% $\delta(\text{S}_2\text{—Cu—N})$ + 28% $\delta(\text{N—Cu—N})$ | 162 | 45% $\delta(\text{S}_1\text{—Cu—N})$ + 41% $\delta(\text{N—Cu—N})$ + 9% $\nu(\text{Cu—S}_1)$ |
| 137 vw | 147 | 49% $\delta(\text{S}_2\text{—Cu—N})$ + 45% $\delta(\text{S}_1\text{—Cu—N})$ | 140 | 77% $\delta(\text{S}_1\text{—Cu—O})$ + 14% $\delta(\text{S}_1\text{—Cu—S}_2)$ |
| 115 m | | | 134 | 57% $\delta(\text{S}_2\text{—Cu—N})$ + 40% $\delta(\text{O—Cu—N})$ |
| | 79 | 70% $\delta(\text{S}_1\text{—Cu—S}_2)$ + 25% $\delta(\text{N—Cu—N})$ | 79 | 65% $\delta(\text{S}_1\text{—Cu—S}_2)$ + 13% $\delta(\text{O—Cu—N})$ + 12% $\delta(\text{S}_2\text{—Cu—N})$ |
| | | | 46 | 43% $\delta(\text{O—Cu—N})$ + 29% $\delta(\text{S}_2\text{—Cu—N})$ + 19% $\delta(\text{S}_1\text{—Cu—S}_2)$ |

* Abbreviations as in Table 1.

while giving less than satisfactory results for square planar or trigonal bipyramidal structures. Thus, we are encouraged to proceed to refinements of this approach incorporating recent spectral and structural observations on some blue copper proteins.

The 1.6-Å resolution crystallographic data for oxidized plastocyanin now show that methionine-92 at 2.90 Å from the Cu atom is very likely beyond bonding distance (22). In addition, Penfield *et al.* (36) conclude on the basis of an electronic spectroscopic study of a single crystal of plastocyanin that this methionine contributes insignificantly to the (Cys)S→Cu(II) charge transfer spectrum in the visible region. Furthermore, all resonance Raman spectra of type 1 site proteins exhibit a band near 260 cm⁻¹, even stellacyanin which lacks methionine altogether. We have also observed the ≈260-cm⁻¹ band in the resonance Raman spectrum (unpublished results) of copper-substituted alcohol dehydrogenase (37), a pseudo blue copper protein in which the copper is located at the catalytic zinc site which is coordinated to one histidine, two cysteines, and one water molecule (38). In addition, we have studied azurin obtained from a *P. aeruginosa* auxotroph grown in selenomethionine, in which methionine-121 was replaced by selenomethionine. We found that the resonance Raman spectra of native and selenium-substituted azurin are indistinguishable (unpublished results). We conclude that complexation of S(Met) by Cu(II) in oxidized azurin is unlikely and that the ≈260-cm⁻¹ vibration in type 1 site proteins is due to a structural feature other than a Cu(II)—S(thioether) linkage.

The subsequent computation again utilized a three-coordinate CuN₂S model with the copper either 0.5, 0.6, or 0.75 Å above the N₂S plane; however, the Cu—ligand bond lengths were constant as before. The force field was modified only to counteract H(N—Cu—S) reaching an excessive value of 110 N·m⁻¹ (Table 2) by fixing this bending force constant at 50 N·m⁻¹ during refinement. The most satisfactory fit with the observed frequencies was obtained for the 0.75-Å Cu elevation, and the results of this calculation are given in Table 4.

As in the previous trigonal set (Table 1), the data in Table 4 show excellent agreement for the three highest frequencies and each of these bands has some $\nu(\text{Cu—S})$ character which, however, predominates at 369 cm⁻¹. A major departure from the trigonal results in Table 1 is that the 261-cm⁻¹ feature is no longer matched, even though it was one of the four input fre-

quencies. The absence of a calculated peak at 261 cm⁻¹ supports our view that such a feature in the observed spectrum is, in fact, not associated with the CuN₂S skeleton. If the 261-cm⁻¹ feature is deleted from the list of input frequencies, data essentially identical to those shown in Table 4 are obtained. The 261-cm⁻¹ frequency as well as the ≈750-cm⁻¹ frequency seemingly common to all type 1 proteins are well matched in our calculations by $\rho(\text{C—S—Cu—N})$ and $\nu(\text{C—S})$, respectively, by using the Cu and C—S(cysteine) geometry proposed for plastocyanin (36) and force constants of 50 N·m⁻¹ for H(C—S—Cu—N) and 290 N·m⁻¹ for K(C—S). Furthermore, our value of ≈0.75 Å for the Cu elevation above the trigonal plane in azurin is consistent with the plastocyanin value of ≈0.5 Å obtained from single crystal optical and EPR data (36).

In the trigonal model for azurin (Table 4) the three most intense spectral features are each assigned significant contributions from Cu—S as well as Cu—N stretching. Because the

Table 4. Frequencies and band assignments for the CuN₂S trigonal model (Cu 0.75 Å above the N₂S plane) with a modified force field

| Obs., cm ⁻¹ * | Calc., cm ⁻¹ | Assignments |
|--------------------------|-------------------------|---|
| 424 s | 424 | 92% $\nu(\text{Cu—N})$ + 7% $\nu(\text{Cu—S})$ |
| 404 vs | 405 | 71% $\nu(\text{Cu—N})$ + 28% $\nu(\text{Cu—S})$ |
| 369 s | 367 | 63% $\nu(\text{Cu—S})$ + 35% $\nu(\text{Cu—N})$ |
| 343 w | | |
| 302 w | | |
| 275 sh, w | | |
| 261 m | | |
| 218 w | | |
| 194 sh, w | | |
| 183 w | 172 | 99% $\delta(\text{N—Cu—S})$ |
| 158 vw | 163 | 94% $\delta(\text{N—Cu—S})$ |
| 137 vw | | |
| 115 m | | |
| | 90 | 96% $\delta(\text{N—Cu—N})$ |

The initial force constants for this computation are taken as the refined values for the appropriate modes from the tetrahedral case in Table 2, except that the value of H(N—Cu—S) was lowered from 68 to 50 and held fixed during refinement. The final force constants are K(Cu—N) = 110 N·m⁻¹; K(Cu—S) = 180 N·m⁻¹; H(N—Cu—N) = 11 N·m⁻¹; H(N—Cu—S) = 50 N·m⁻¹.

* Abbreviations as in Table 1.

three dominant electronic absorption bands in plastocyanin (and, by analogy, in azurin) are attributed to cysteine→Cu(II) charge-transfer transitions (36), the coupled nature of each of the three vibrational modes provides a mechanism for their resonance enhancements. The observation that the relative intensities of the three major Raman peaks are unaltered when the excitation wavelength is varied from 488.0 to 676.4 nm confirms that these features arise from Franck-Condon overlaps with the cysteine→Cu(II) transitions and are essentially unaffected by the weaker transitions below 480 nm associated with histidine→Cu(II) charge transfer (12, 13, 36). The coupling of the Cu—N and Cu—S vibrations may explain why in the normal coordinate analysis the histidine ligand nitrogen can be treated independently of the imidazole ring. In the type 1 model, *p*-nitrobenzenethiolato(hydrotris(3,5-dimethyl-1-pyrazolyl)borato)copper(II), the assigned Cu—N vibrations at 339, 360, and 385 cm⁻¹ are also anomalously high for imidazole-like ν (Cu—N) (39). It is probable that these, too, represent coupled vibrations in a constrained tetrahedral coordination geometry. In contrast, in the unconstrained tetrahedral dihalobis(imidazole) Zn(II) complexes in which all four ligands appear to have uncoupled vibrations, the normal coordinate analysis gives a best fit by treating the imidazoles as rigid vibrators with a mass of 68 atomic mass units (34).

The assignment of the 424-cm⁻¹ peak in azurin to a predominantly Cu—N vibration is in accord with its lack of contribution to the overtone bands discussed above (5). The determination that the largest ν (Cu—S) contribution is in the peak at 369 cm⁻¹ in azurin agrees with the findings from the resonance Raman spectrum of the Cu(II)-substituted alcohol dehydrogenase (37) which has intense peaks at 415 and \approx 360 cm⁻¹ (unpublished results). The \approx 360-cm⁻¹ band is generally asymmetric and both its shape and frequency are dependent upon the nature of added substrates. Because the catalytic zinc ion is coordinated to two cysteines and a histidine in the native enzyme (38), the components contributing the \approx 360-cm⁻¹ band appear to be due to the two (Cu—S) vibrations and the 415-cm⁻¹ peak is due to ν (Cu—N) in the Cu(II)-alcohol dehydrogenase.

SUMMARY

A critical analysis of the calculated frequencies and force fields as a function of the copper—ligand structure supports a tetrahedral CuN₂SS' or a trigonal CuN₂S description of the site over square planar or trigonal bipyramidal models. Evidence is presented in favor of the trigonal CuN₂S(Cys) description of the azurin center. The trigonal model that best fits calculated frequencies to the observed resonance Raman frequencies has the Cu atom \approx 0.75 Å above the N₂S plane and assigns the three highest frequency peaks to coupled Cu—N and Cu—S stretching vibrations. The \approx 260-cm⁻¹ peak observed in the resonance Raman spectra of all blue copper proteins and which had generally been ascribed to a Cu—S(Met) bond vibration is reassigned to a Cu—S—C deformation mode of the coordinated cysteine. These structural predictions extend the basis of similarity of azurin with the active site of plastocyanin and provide detailed descriptions of the assignment of the resonance Raman spectra of blue copper proteins.

We thank Joann Sanders-Loehr and Thomas G. Spiro for helpful discussions. We are grateful to the National Institutes of Health for support of this research (GM 18865).

1. Siiman, O., Young, N. M. & Carey, P. R. (1974) *J. Am. Chem. Soc.* **96**, 5583–5585.

2. Miskowski, V., Tang, S.-P. W., Spiro, T. G., Shapiro, E. & Moss, T. H. (1975) *Biochemistry* **14**, 1244–1250.
3. Tosi, L., Garnier, A., Hervé, M. & Steinbuch, M. (1975) *Biochem. Biophys. Res. Commun.* **65**, 100–105.
4. Siiman, O., Young, N. M. & Carey, P. R. (1976) *J. Am. Chem. Soc.* **98**, 744–748.
5. Ferris, N. S., Woodruff, W. H., Tennent, D. L. & McMillin, D. R. (1979) *Biochem. Biophys. Res. Commun.* **88**, 288–296.
6. McMillin, D. R., Rosenberg, R. C. & Gray, H. B. (1974) *Proc. Natl. Acad. Sci. USA* **71**, 4760–4762.
7. Markley, J. L., Ulrich, E. L., Berg, S. P. & Krogmann, D. W. (1975) *Biochemistry* **14**, 4428–4433.
8. Adman, E. T. & Jensen, L. H. (1981) *Isr. J. Chem.* **21**, 8–12.
9. Colman, P. M., Freeman, H. C., Guss, J. M., Murata, M., Norris, V. A., Ramshaw, J. A. M. & Venkatappa, M. P. (1978) *Nature (London)* **272**, 319–324.
10. Tullius, T. D., Frank, P. & Hodgson, K. O. (1978) *Proc. Natl. Acad. Sci. USA* **75**, 4069–4073.
11. Peisach, J. & Mims, W. B. (1978) *Eur. J. Biochem.* **84**, 207–214.
12. Solomon, E. I., Hare, J. W., Dooley, D. M., Dawson, J. H., Stephens, P. J. & Gray, H. B. (1980) *J. Am. Chem. Soc.* **102**, 168–178.
13. Gray, H. B. & Solomon, E. I. (1981) *Met. Ions Biol.* **3**, 1–39.
14. Freedman, T. B., Loehr, J. S. & Loehr, T. M. (1976) *J. Am. Chem. Soc.* **98**, 2809–2815.
15. Eickman, N. C., Solomon, E. I., Larrabee, J. A., Spiro, T. G. & Lerch, K. (1978) *J. Am. Chem. Soc.* **100**, 6529–6531.
16. Adams, D. M. & Cornell, J. B. (1967) *J. Chem. Soc.*, 884–889.
17. Tosi, L. & Garnier, A. (1978) *J. Chem. Soc. Dalton Trans.*, 53–56.
18. Siiman, O. & Carey, P. R. (1980) *J. Inorg. Biochem.* **12**, 353–362.
19. Tosi, L. & Garnier, A. (1979) *Biochem. Biophys. Res. Commun.* **91**, 1273–1279.
20. Ferris, N. S., Woodruff, W. H., Rorabacher, D. B., Jones, T. E. & Ochrymowycz, L. A. (1978) *J. Am. Chem. Soc.* **100**, 5939–5942.
21. Bergman, C., Gandvik, E.-K., Nyman, P. O. & Strid, L. (1977) *Biochem. Biophys. Res. Commun.* **77**, 1052–1059.
22. Freeman, H. C. (1981) in *Coordination Chemistry—21*, ed. Laurent, J. P. (Pergamon, Oxford), pp. 29–51.
23. Ambler, R. P. & Wynn, M. (1973) *Biochem. J.* **131**, 485–498.
24. Parr, S. R., Barber, D., Greenwood, C., Philips, B. W. & Mellinger, J. (1976) *Biochem. J.* **157**, 423–430.
25. Loehr, T. M., Keyes, W. E. & Pincus, P. A. (1979) *Anal. Biochem.* **96**, 456–463.
26. Wilson, E. B., Jr. (1939) *J. Chem. Phys.* **7**, 1047–1052.
27. Fuhrer, H., Kartha, V. B., Krueger, P. J., Mantsch, H. H. & Jones, R. N. (1972) *Chem. Rev.* **72**, 439–456.
28. Fuhrer, H., Kartha, V. B., Kidd, K. G., Krueger, P. J. & Mantsch, H. H. (1976) *Computer Programs for Infrared Spectrophotometry* (National Research Council of Canada, Ottawa, ON), Vol. 5, Bull. No. 15.
29. Thamann, T. J. & Loehr, T. M. (1981) *Spectrochim. Acta Part A* **36**, 751–760.
30. Armendarez, P. X. & Nakamoto, K. (1966) *Inorg. Chem.* **5**, 796–800.
31. Nakamoto, K., Fujita, J., Condrate, R. A. & Morimoto, Y. (1963) *J. Chem. Phys.* **39**, 423–427.
32. Durga Prasad, G., Sathyanarayana, D. N. & Patel, C. C. (1969) *Can. J. Chem.* **47**, 631–635.
33. Ray, A., Sathyanarayana, D. N., Durga Prasad, G. & Patel, C. C. (1973) *Spectrochim. Acta Part A* **29**, 1579–1584.
34. Cornilsen, B. C. & Nakamoto, K. (1974) *J. Inorg. Nucl. Chem.* **36**, 2467–2471.
35. Ugurbil, K., Norton, R. S., Allerhand, A. & Bersohn, R. (1977) *Biochemistry* **16**, 886–894.
36. Penfield, K. W., Gay, R. R., Himmelwright, R. S., Eickman, N. C., Norris, V. A., Freeman, H. C. & Solomon, E. I. (1981) *J. Am. Chem. Soc.* **103**, 4382–4388.
37. Maret, W., Dietrich, H., Ruf, H.-H. & Zeppezauer, M. (1980) *J. Inorg. Biochem.* **12**, 241–252.
38. Brändén, C.-I., Jörnvall, H., Eklund, H. & Furugren, B. (1975) in *The Enzymes*, ed. Boyer, P. (Academic, New York), Vol. 11, pp. 103–190.
39. Thompson, J. S., Marks, T. J. & Ibers, J. A. (1979) *J. Am. Chem. Soc.* **101**, 4180–4192.